

University of Groningen

Phase locking of a 3.4 THz third-order distributed feedback quantum cascade laser using a room-temperature superlattice harmonic mixer

Hayton, D. J.; Khudchencko, A.; Pavelyev, D. G.; Hovenier, J. N.; Baryshev, A.; Gao, J. R.; Kao, T. Y.; Hu, Q.; Reno, J. L.; Vaks, V.

Published in:
Applied Physics Letters

DOI:
[10.1063/1.4817319](https://doi.org/10.1063/1.4817319)

IMPORTANT NOTE: You are advised to consult the publisher's version (publisher's PDF) if you wish to cite from it. Please check the document version below.

Document Version
Publisher's PDF, also known as Version of record

Publication date:
2013

[Link to publication in University of Groningen/UMCG research database](#)

Citation for published version (APA):

Hayton, D. J., Khudchencko, A., Pavelyev, D. G., Hovenier, J. N., Baryshev, A., Gao, J. R., Kao, T. Y., Hu, Q., Reno, J. L., & Vaks, V. (2013). Phase locking of a 3.4 THz third-order distributed feedback quantum cascade laser using a room-temperature superlattice harmonic mixer. *Applied Physics Letters*, 103(5), [051115]. <https://doi.org/10.1063/1.4817319>

Copyright

Other than for strictly personal use, it is not permitted to download or to forward/distribute the text or part of it without the consent of the author(s) and/or copyright holder(s), unless the work is under an open content license (like Creative Commons).

The publication may also be distributed here under the terms of Article 25fa of the Dutch Copyright Act, indicated by the "Taverne" license. More information can be found on the University of Groningen website: <https://www.rug.nl/library/open-access/self-archiving-pure/taverne-amendment>.

Take-down policy

If you believe that this document breaches copyright please contact us providing details, and we will remove access to the work immediately and investigate your claim.

Downloaded from the University of Groningen/UMCG research database (Pure): <http://www.rug.nl/research/portal>. For technical reasons the number of authors shown on this cover page is limited to 10 maximum.



AIP Applied Physics Letters

HOME

ISSUES

MORE ▼

[Home](#) > [Applied Physics Letters](#) > [Volume 103, Issue 5](#) > [10.1063/1.4817319](#)



< PREV

NEXT >

Full

Published Online: August 2013

Accepted: July 2013

Phase locking of a 3.4 THz third-order distributed feedback quantum cascade laser using a room-temperature superlattice harmonic mixer

Appl. Phys. Lett. **103**, 051115 (2013); <https://doi.org/10.1063/1.4817319>

D. J. Hayton^{1, a)}, A. Khudchenko¹, D. G. Pavelyev², J. N. Hovenier³, A. Baryshev¹, J. R. Gao^{1,3, b)}, T. Y. Kao⁴, Q. Hu⁴, J. L. Reno⁵, and V. Vaks⁶

[View Affiliations](#)





Topics ▾

- Correction: [Appl. Phys. Lett. 103, 109903 \(2013\)](#)

ABSTRACT

We report on the phase locking of a 3.4 THz third-order distributed feedback quantum cascade laser (QCL) using a room temperature GaAs/AlAs superlattice diode as both a frequency multiplier and an internal harmonic mixer. A signal-to-noise level of 60 dB is observed in the intermediate frequency signal between the 18th harmonic of a 190.7 GHz reference source and the 3433 GHz QCL. A phase-lock loop with 7 MHz bandwidth results in QCL emission that is 96% locked to the reference source. We characterize the QCL temperature and electrical tuning mechanisms and show that frequency dependence of these mechanisms can prevent phase-locking under certain QCL bias conditions.

Since the development of the first THz quantum cascade lasers (QCLs),¹ there has been considerable progress made in their development. They are compact and offer lasing at any frequency between roughly 1 and 5 THz with high output power in the range of tens of milliwatts, making them highly suitable for many applications from local oscillator (LO) sources for high resolution heterodyne spectroscopy to gas sensing and terahertz imaging.

One of the key applications driving the development of the THz QCL is heterodyne spectroscopy in the super-terahertz which is loosely



defined as 2 to 6 THz. For frequencies beyond 2 THz, there are few solid state sources available. The commonly used LO below 2 THz is the multiplier based source which, to date, has demonstrated output power of a microwatt at up to 2.7 THz. For an LO source, single mode emission is crucial. A 3rd order distributed feedback (DFB) laser, as to be explained, can offer not only a robust single mode operation, but also a relatively narrow single-lobe beam. The latter is of practical importance for efficient coupling of the radiation to a mixer or mixer array.

Frequency locking of a THz QCL was first demonstrated by Betz *et al.*² in 2005. Since then, it has been well established that to apply a QCL as an LO in a real receiver system, either frequency stabilization or phase locking is required. For this reason, many frequency or phase locking experiments have been reported in the literature. Those demonstrations can be mainly divided into a few cases: (a) phase locking of Fabry-Perot (FP) based QCLs with the use of a cooled superconducting detector as the mixing element³⁻⁵ or by the use of a frequency comb generated from a mode-lock femtosecond laser.^{6,7} The latter is operated at room temperature but requires relatively bulky and high power consumption electronics; (b) frequency locking of an FP or 3rd order DFB laser using a gas absorption line as the reference;⁸ (c) frequency locking of an FP laser using a Schottky-diode harmonic mixer,⁹ which was operated at room temperature, but requires high THz input power from the QCL in the order of several mW and has so far been demonstrated only below 3 THz.

In this paper we report on a phase locking demonstration of a 3.4 THz 3rd order DFB laser QCL using a room-temperature component, which is a GaAs/AlAs superlattice device that serves simultaneously as a

previous work, the present scheme does not require a cryogenic detector, is much more compact, and can achieve phase locking at >3 THz. The intermediate frequency (IF) signal for the phase locking loop is the result of mixing between the internally generated 18th harmonic of a 190.7 GHz reference source and the QCL signal. We demonstrated the phase locking not only by observing the narrow IF linewidth, but also by measuring the phase locking efficiency. Just as importantly, we also find that for this 3rd order DFB laser, the phase locking is possible only under certain QCL bias conditions, revealing details of two competing tuning mechanisms.

In contrast with the QCLs in previous phase locking experiments, the QCL used here adopts a frequency selective mechanism in the form of a 3rd order DFB laser grating structure^{10,11} that forces single mode emission while retaining a degree of tunability. This recent introduction of the 3rd order DFB laser represents a significant step forward in QCL design in terms of practical application. The DFB grating structure makes use of the constructive interference of radiation emitted from each unit of the grating and thus acts as an end-fire linear $\lambda/2$ antenna array. In addition to the robust single-mode emission frequency control, DFB QCLs also show a single lobe, less divergent beam with a spherical wavefront,¹² which leads to an improvement in optical efficiency. The QCL used here has single mode emission at ~ 3.4 THz and is designed and fabricated at MIT (sample FS183S-VA0094). It is based on the four-well resonant-phonon depopulation design.¹³ The device comprises a 10 μm thick, 17 μm wide active region of MBE grown GaAs/AlGaAs with 27 lateral corrugated grating periods over the 1.07 mm length of the laser. The measured total THz CW output power is about 1 mW and the DC power dissipation is 3 W when operating at ~ 15 to 20 K.

We used a GaAs/AlAs superlattice harmonic frequency mixer based on nonlinear miniband transport¹⁴ to generate a harmonic of the reference in the vicinity of the QCL frequency, the same nonlinearity is also used as a mixer for phase locking. The harmonic multiplier/mixer consists of a superlattice planar diode mounted between two opposing waveguides. These waveguides serve as inputs for both the 100–200 GHz mixer LO (for the harmonic mixer) via a fin-line, and the THz signal via a diagonal feedhorn with an upper frequency cutoff at ~ 6.5 THz.¹⁵ The superlattice structure is grown by molecular beam epitaxy on an intrinsic GaAs substrate. It comprises an n+ GaAs layer (thickness $1.5\ \mu\text{m}$; doping $6 \times 10^{18}\ \text{cm}^{-3}$), a GaAs/AlAs gradual layer (thickness 32 nm), then the superlattice, again a gradual layer and n+ GaAs and an n+ InGaAs gradual layer (25 nm) and finally an n+ InGaAs layer (20 nm, doping $10^{19}\ \text{cm}^{-3}$) serving as the ohmic contact. The superlattice (length 112 nm) has 18 periods, each period (length 6.22 nm) with 18 monolayers GaAs and 4 monolayers AlAs and was homogeneously doped with silicon ($2 \times 10^{18}\ \text{cm}^{-3}$). The mixer requires no external bias input and the IF is output via an SMA connector. This structure provides a relatively low conversion loss for a room temperature mixer (~ 80 dB), leading to a phase-lock loop (PLL) system without the need for a cooled superconducting mixer.

The phase locking experimental setup is shown in Figure 1. Also indicated by the dashed line is an additional setup used to implement a frequency lock loop. In this configuration it is possible to select phase or frequency locking by nulling the loop gain of the loop not in use.

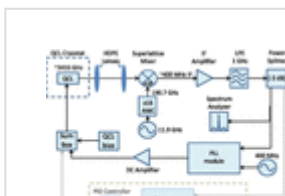


FIG. 1.

Schematic of the setup for phase locking. An additional frequency lock loop is indicated within the dashed box.

↓ PPT | High-resolution

The QCL was operated in a liquid helium flow cryostat with a 1.2 mm high-density polyethylene (HDPE) cryostat window. Its THz radiation is optically coupled into the harmonic mixer through two room temperature HDPE lenses that are used in a standard telescopic type configuration to focus the THz radiation onto the harmonic mixer feedhorn. The frequency of this laser is chosen to coincide with an atmospheric transmission window so that the losses in air are minimal. The harmonic mixer is pumped with an 8 mW, 190.744 GHz LO source provided by an amplifier-multiplier-chain (AMC) source from Virginia Diodes.¹⁶ This AMC chain is a quad-doubler ($\times 16$) system that is driven by an 11.92 GHz R&S microwave synthesizer. The 18th harmonic of the LO source at 3433.4 GHz is combined with the ~ 3433 GHz QCL emission by the superlattice mixer, resulting in a ~ 400 MHz beat note with ~ 60 dB of signal to noise. This IF signal is amplified by multi-stage room temperature amplifiers with a total gain of 26 dB and is filtered using a 1 GHz low pass edge (LPE) filter before passing through a pick-off coupler for output to an RF spectrum analyzer. The signal is then divided using a 3 dB power splitter between the phase and frequency detector elements. The loops are completed by combining the phase (or frequency) feedback signals with the QCL DC bias (14–16 V from an Agilent PSU)

using a wide bandwidth (DC to 20 MHz) signal summing box. The output of the summing box supplies bias directly to the QCL.

The phase error signal is generated by a wideband PLL module,¹⁷ which has a bandwidth of 40 MHz and an adjustable loop gain. An integrating filter, located after the phase detector, provides a stable second-order PLL. The feedback output signal from the PLL is further amplified by two room temperature amplifiers with a response from DC to 7 MHz. These amplifiers limit the bandwidth of the overall phase-locking loop to 7 MHz, which is more than sufficient for QCL phase locking in our case, but can be increased if necessary.

Observation of the IF signal using a spectrum analyzer provides a very fast and precise way of measuring the QCL emission frequency. This method was initially used to characterize the frequency versus bias voltage for this QCL so that we may verify its operation as a voltage controlled oscillator; the fundamental requirement for phase/frequency locking. This laser has a tuning range of ~3431.75 to 3433.80 GHz over a bias range from 13.8 to 15.8 V, which was measured at a constant bath temperature of 25 K (Fig. 2, main plot) by carefully controlling the L-He flow for each bias point. We see that at 14.5 V, the tuning coefficient reverses sign and remains positive up to the highest bias. To explain the nonmonotonic tuning behavior, it is necessary to describe the tuning mechanisms within the QCL. The emission wavelength of a 3rd order DFB QCL is primarily defined by $2dn/3$, where d is the grating period and n the effective refractive index of the laser. The emission frequency is therefore principally determined by the effective refractive index which, in turn, is determined by (a) its temperature, which causes red shift tuning for increasing bias and (b) the so-called Stark effect in which

presence of an electric field resulting in a change of absorption frequency which, through the Kramers–Kronig relation, induces a corresponding change in refractive index. The Stark effect can result in a red shift or a blue shift, depending on the relative energy alignment of the involved sub-band levels^{18,19} and it is responsible for the change in sign of the tuning coefficient that we observe at 14.5 V. In practice, adjustment of the QCL bias voltage also varies the temperature in the QCL due to the change in dissipated power, so a combination of the tuning mechanisms is expected. Typically electrical and thermal tuning coefficients for this QCL are 1490 MHz/V at 15 V, 25 K and -161 MHz/K at 15 V, 25 K, respectively (the equivalent current tuning coefficient is 27 MHz/mA). The reverse in the bias tuning coefficient combined with the anti-correlation of the tuning mechanisms will have strong implications for phase locking that are discussed later.

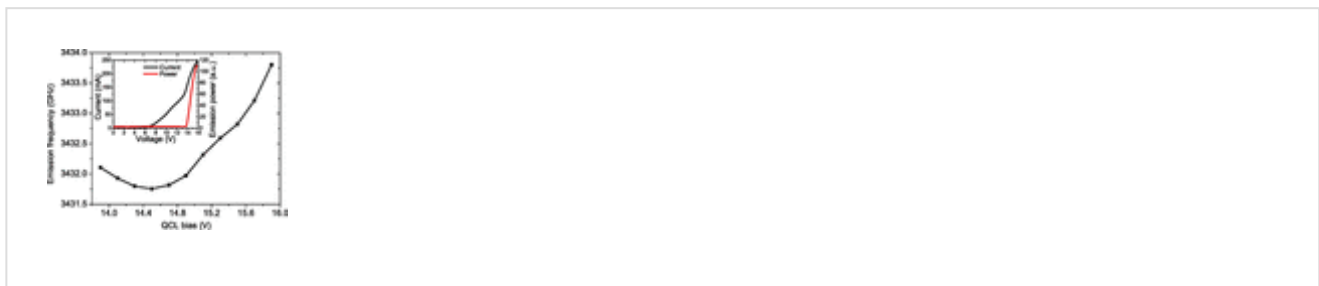


FIG. 2.

QCL CW emission frequency versus bias voltage at a bath temperature of 25 K. Frequency is measured using the superlattice harmonic mixer. The inset shows current and relative emission power versus voltage for the QCL used in this work.

↓ PPT | High-resolution

↓ PDF

While the main focus of this letter is QCL phase locking, it is worthwhile to note that frequency locking is relatively straightforward to implement with the superlattice mixer and, unlike the commonly used technique of locking to a molecular absorption line,⁸ it can easily provide locking at any frequency in the QCL tuning range. The setup for the frequency lock loop is indicated in Fig. 1. It is achieved using a frequency detector module that produces, via a frequency discriminator, an output voltage proportional to the mixer IF signal frequency relative to an internal 400 MHz reference over an IF bandwidth of 140 MHz. In this way, the QCL locking frequency can be chosen by selecting the appropriate harmonic mixer LO frequency that results in an IF at ± 400 MHz. The feedback signal is generated by a hardware proportional-integral-derivative (PID) controller with 100 kHz loop bandwidth (model: SRS-SIM960). In this configuration, the QCL bias is adjusted by the PID controller to maintain the set point frequency. Excellent frequency locking results were observed even when operating the QCL within a relatively thermally unstable L-He flow cryostat for which a constant drift in bath temperature is difficult to avoid. Frequency locking was possible over practically all of the QCLs bias range with the exception of a very narrow bias region centered around 14.5 V (see Figure 2) in which the frequency tuning coefficient approaches zero. The measured frequency locked linewidth spectrum displays a Lorentz profile with 48 kHz width. This linewidth is in good agreement with the 51 kHz measured using the frequency locking based on a molecular absorption line in Ref. 8. It should be noted that both linewidth measurements employ the same PID controller with a loop bandwidth of 100 kHz. It is interesting to note that the measured frequency locked linewidth is at least one order of magnitude larger than the extracted intrinsic linewidth derived from the

linewidth in our case can be attributed primarily to the loop bandwidth, which is unable to suppress the frequency noise beyond 100 kHz, but also more fundamental differences in the QCL itself (i.e., use of resonant-phonon over single-plasmon bound-to-continuum design and DFB over FP frequency selection mechanism).

The result of the QCL phase locking is represented in Fig. 3 by a spectrum of the phase-locked IF signal at spectrometer resolution bandwidths of 100 kHz and 1 Hz. We show that the spectrum demonstrates a high degree of phase locking with 96% of the QCL radiation power locked to the reference, up-converted from the microwave synthesizer. This number was calculated using the method described in Ref. 21 as the ratio of the power locked in a central peak of the spectrum to the total coupled power including the phase noise, integrated from 1 Hz to 20 MHz and in which the IF noise level was separately measured and subtracted. The phase noise peaks visible on either side of the main peak in Figure 3 point to a PLL bandwidth of about 7 MHz which is in good agreement with the bandwidth of our IF amplifier. Since the central peak of the synchronized QCL should be extremely narrow we measured a phase noise distribution down to 1 Hz frequency offset from the carrier (Fig. 3). From Fig. 3, one can see the phase noise to be very low, typically at a level of about -80 dB relative to the carrier [or dBc] (recalculated to 1 Hz resolution bandwidth).

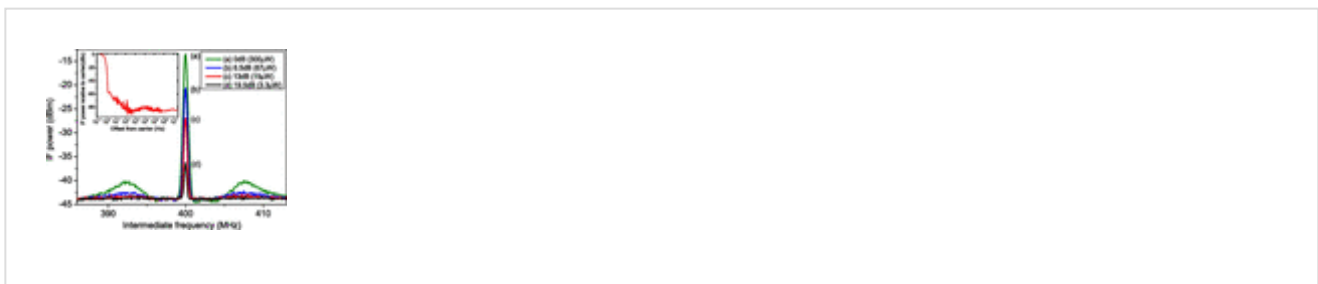


FIG. 3.

Power spectrum of the IF beat signal for the phase locked system measured with a spectrometer resolution bandwidth of 100 kHz. IF spectra are shown with increasing optical attenuation. The inset shows the residual phase noise relative to the carrier for the phase locked system adjusted to 1 Hz resolution bandwidth.

[↓ PPT](#) | [High-resolution](#)

Using an absolute power meter (Erickson PM4) in place of the mixer, we estimate the THz incident power entering the superlattice waveguide to be $\sim 300 \mu\text{W}$. By measuring incident power in the same way, and by optically attenuating the QCL, we observe that phase locking is possible down to a superlattice incident power of $\sim 3.3 \mu\text{W}$ (Fig. 3) showing that this PLL system requires only a small fraction of the output power from a typical QCL, making it to be practical for operation.

Interestingly, we discovered that phase locking is not possible over the full bias range of this QCL, but only possible for the positive slope of the frequency-bias curve, or at bias $>14.5 \text{ V}$, as shown in Figure 2. For bias levels below 14.5 V, where the tuning coefficient is negative, phase locking is not possible. In this case, the effect of the PLL is opposite to that expected. As the PLL gain is increased, the QCL linewidth is broadened and the frequency is pushed away from the reference, despite the PLL having no dependence on the sign of the frequency tuning coefficient. This can be explained by considering the different time constants and anti-correlation of the temperature and electrical tuning mechanisms. Temperature tuning is a relatively slow process

thermal time constant of the QCL, $\tau = C/G$, where C is the heat capacity and G the thermal conductance. Stark electrical tuning however is a very fast process limited only by the RC time constant of the QCL which is typically on the order of pico seconds.¹⁸ To examine this further, we devise a test to observe the bias frequency dependence in the regions both above and below 14.5 V by applying a square wave modulation ($\Delta V_{pp} = 4$ mV) to the QCL bias voltage. This bias modulation translates into frequency modulation of the QCL emission corresponding to the two bias levels. We then use the harmonic mixer to accurately measure the magnitude of the frequency modulation (Δf) and calculate the tuning coefficient ($\Delta f/\Delta V$) as a function of the modulation frequency from a few Hz to a few hundred kHz (Fig. 4). In the lower QCL bias regime ($V_{bias} = 14.0$ V in Fig. 2), where temperature tuning dominates over Stark tuning at low modulation frequencies, we observe that, as the bias frequency increases and the magnitude of the temperature tuning diminishes, a change in the sign of the tuning coefficient occurs at a bias frequency of 50 kHz. In this case, the temperature and Stark tuning coefficients are equal and opposite at 50 kHz resulting in a tuning coefficient equal to zero. It is this inversion in the sign of the tuning coefficient occurring at bias voltages <14.5 V that prevents phase locking. In contrast, as the bias level increases above 14.5 V, electrical tuning becomes stronger and dominates, leading to a positive tuning coefficient over all modulation frequencies. At this higher bias level, the temperature tuning effect is still present since the tuning coefficient increases at approximately the same rate with increasing modulation frequency however, at no point is it stronger than the electric Stark tuning. In this regime, phase locking was observed. With this, we can conclude that for successful phase locking, a QCL gain medium should

be engineered such that Stark tuning dominates in the intended bias range of a particular device.

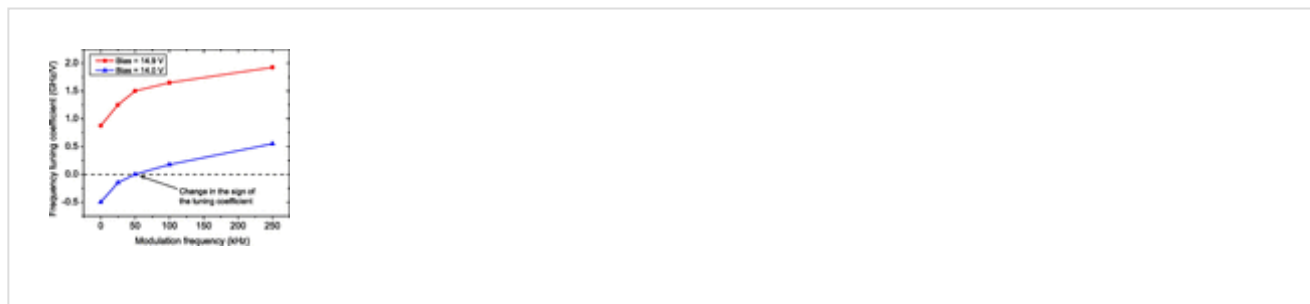


FIG. 4.

QCL frequency tuning coefficient versus bias modulation frequency for two QCL bias levels.

[↓ PPT](#) | [High-resolution](#)

In conclusion, we have demonstrated both the frequency and phase locking of a 3rd order DFB QCL using a room temperature superlattice harmonic mixer. The high efficiency of our mixer yields ~60 dB of signal-to-noise in the IF from only 300 μ W of coupled 3433 GHz QCL power. We show a PLL bandwidth of 7 MHz with 96% of QCL power phase locked to the reference. The superlattice harmonic mixer can be easily and effectively applied in a frequency lock loop by including a frequency detector and PID controller in the system. We also demonstrate a unique method of bias modulation to characterize the frequency dependence of several QCL tuning mechanisms. As a result, we identify and explain why certain bias conditions are not suitable for phase locking. Ultimately, this knowledge can lead to improvements in QCL design for phase locking applications.

We acknowledge Y Ren for his extensive past work in characterizing this QCL and W. Horinga and B. Kramer for their technical support. The work in the Netherlands was supported by NWO, Teradec, the AETHER of RadioNet under FP7, and NATO SFP. The work at MIT is supported by NASA and NSF. The work at Sandia was performed, in part, at the Center for Integrated Nanotechnologies, a U.S. Department of Energy, Office of Basic Energy Sciences user facility. Sandia National Laboratories is a multiprogram laboratory managed and operated by Sandia Corporation, a wholly owned subsidiary of Lockheed Martin Corporation, for the U.S. Department of Energy National Nuclear Security Administration under contract DE-AC04-94AL85000. The work in Russia has been supported by the Russian Foundation of Basic Research (Grant No. N11-02-12124 - офи-м).

REFERENCES

1.

R. Köhler, A. Tredicucci, F. Beltram, H. E. Beere, E. H. Linfield, A. G. Davies, D. A. Ritchie, R. C. Iotti, and F. Rossi, *Nature* **417**, 156 (2002).

<https://doi.org/10.1038/417156a> , [Google Scholar](#), [Crossref](#) [Open URL](#)

2.

A. L. Betz, R. T. Boreiko, B. S. Williams, S. Kumar, Q. Hu, and J. L. Reno, *Opt. Lett.* **30**, 1837 (2005). <https://doi.org/10.1364/OL.30.001837> ,

[Google Scholar](#), [Crossref](#), [CAS](#) [Open URL](#)

3.

A. Baryshev, J. N. Hovenier, A. J. L. Adam, I. Kašalynas, J. R. Gao, T. O. Klaassen, B. S. Williams, S. Kumar, Q. Hu, and J. L. Reno, Appl. Phys. Lett. **89**, 031115 (2006). <https://doi.org/10.1063/1.2227624> , [Google Scholar](#), [Scitation](#) [Open URL](#)

4.
D. Rabanus, U. U. Graf, M. Philipp, O. Ricken, J. Stutzki, B. Vowinkel, M. C. Wiedner, C. Walther, M. Fischer, and J. Faist, Opt. Express **17**, 1159 (2009). <https://doi.org/10.1364/OE.17.001159> , [Google Scholar](#), [Crossref](#), [CAS](#) [Open URL](#)

5.
P. Khosropanah, A. Baryshev, W. Zhang, W. Jellema, J. N. Hovenier, J. R. Gao, T. M. Klapwijk, D. G. Paveliev, B. S. Williams, S. Kumar, Q. Hu, J. L. Reno, B. Klein, and J. L. Hesler, Opt. Lett. **34**, 2958 (2009). <https://doi.org/10.1364/OL.34.002958> , [Google Scholar](#), [Crossref](#), [CAS](#) [Open URL](#)

6.
L. Consolino, A. Taschin, P. Bartolini, S. Bartalini, P. Cancio, A. Tredicucci, H. E. Beere, D. A. Ritchie, R. Torre, M. S. Vitiello, and P. De Natale, Nat. Commun. **3**, 1040 (2012). <https://doi.org/10.1038/ncomms2048> , [Google Scholar](#), [Crossref](#), [CAS](#) [Open URL](#)

7.

M. Ravaro, C. Manquest, C. Sirtori, S. Barbieri, G. Santarelli, K. Blary, J. F. Lampin, S. P. Khanna, and E. H. Linfield, Opt. Lett. **36**, 3969 (2011).

<https://doi.org/10.1364/OL.36.003969> , [Google Scholar](#), [Crossref](#), [CAS](#)

[Open URL](#)

8.

Y. Ren, J. N. Hovenier, M. Cui, D. J. Hayton, J. R. Gao, T. M. Klapwijk, S. C. Shi, T.-Y. Kao, Q. Hu, and J. L. Reno, Appl. Phys. Lett. **100**, 041111 (2012).

<https://doi.org/10.1063/1.3679620> , [Google Scholar](#), [Scitation](#) [Open URL](#)

9.

A. Danylov, A. Light, J. Waldman, N. Erickson, X. Qian, and W. Goodhue, Opt. Express **20**, 27908 (2012). <https://doi.org/10.1364/OE.20.027908> ,

[Google Scholar](#), [Crossref](#) [Open URL](#)

10.

M. I. Amanti, G. Scalari, F. Castellano, M. Beck, and J. Faist, Opt. Express **18**, 6390 (2010). <https://doi.org/10.1364/OE.18.006390> , [Google Scholar](#),

[Crossref](#), [CAS](#) [Open URL](#)

11.

T.-Y. Kao, Q. Hu, and J. L. Reno, Opt. Lett. **37**, 2070 (2012).

<https://doi.org/10.1364/OL.37.002070> , [Google Scholar](#), [Crossref](#)

[Open URL](#)

12.

M. Cui, J. N. Hovenier, Y. Ren, N. Vercruyssen, J. R. Gao, T. Y. Kao, Q. Hu, and J. L. Reno, Appl. Phys. Lett. **102**, 111113 (2013).

<https://doi.org/10.1063/1.4798250> , [Google Scholar](#), [Scitation](#) [Open URL](#)

13.

Q. Qin, B. S. Williams, S. Kumar, J. L. Reno, and Q. Hu, Nat. Photonics **3**, 732 (2009). <https://doi.org/10.1038/nphoton.2009.218> , [Google Scholar](#), [Crossref](#), [CAS](#) [Open URL](#)

14.

D. G. Paveliev, Y. I. Koshurinov, A. S. Ivanov, A. N. Panin, V. L. Vax, V. I. Gavrilenko, A. V. Antonov, V. M. Ustinov, and A. E. Zhukov, Semiconductors **46**, 125 (2012). <https://doi.org/10.1134/S1063782612010150> , [Google Scholar](#), [Crossref](#) [Open URL](#)

15.

A. N. Panin, V. L. Vaks, Y. I. Koshurinov, and D. G. Paveliev, “ Generation of harmonics up to frequency 6.5 THz with using of frequency multiplier on quantum semiconductor superlattices,” in Proceedings of IRMMW-THz2009, Korea, 2009. [Google Scholar](#), [Open URL](#)

16.

Virginia Diodes Inc., 979 2nd Street SE, Suite 309 Charlottesville, Virginia 22902, USA. [Google Scholar](#)

17.

V. Vaks, A. Illiyuk, A. Panin, S. Pripolsin, S. Basov, and D. Paveliev, in Proceedings of the 37th European Microwave Conference (2007), p.

[Google Scholar](#), [Open URL](#)

18.

M. Pantouvaki, C. C. Renaud, P. Cannard, M. J. Robertson, R. Gwilliam, and A. J. Seeds, IEEE J. Sel. Top. Quantum Electron. **13**, 1112 (2007).

<https://doi.org/10.1109/JSTQE.2007.906046> , [Google Scholar](#), [Crossref](#), [CAS](#) [Open URL](#)

19.

T. Y. Kao, Simulations of Stark induced refractive index versus bias for a 3.4 THz DFB QCL show a similar trend to the one observed however more accurate simulations for this exact QCL are not possible without precise knowledge of the laser gain spectrum at each bias point. This cannot be measured after formation of the DFB grating (unpublished).

[Google Scholar](#), [Open URL](#)

20.

M. S. Vitiello, L. Consolino, S. Bartalini, A. Taschin, A. Tredicucci, M. Inguscio, and P. D. Natale, Nat. Photonics **6**, 525 (2012).

<https://doi.org/10.1038/nphoton.2012.145> , [Google Scholar](#), [Crossref](#), [CAS](#) [Open URL](#)

21.

G. Santarelli, A. Clairon, S. N. Lea, and G. M. Tino, Opt. Commun. **104**, 339 (1994). [https://doi.org/10.1016/0030-4018\(94\)90567-3](https://doi.org/10.1016/0030-4018(94)90567-3) ,

[Google Scholar](#), [Crossref](#), [CAS](#) [Open URL](#)



© 2013 AIP Publishing LLC.

Resources

AUTHOR

LIBRARIAN

ADVERTISER

General Information

ABOUT

CONTACT

HELP

PRIVACY POLICY

TERMS OF USE

FOLLOW AIP PUBLISHING:



Website © 2018 AIP Publishing LLC. Article copyright remains as specified within the article.

Scitation

